The treatment of classically forbidden electronic transitions in semiclassical trajectory surface hopping calculations

Ahren W. Jasper, Michael D. Hack, and Donald G. Truhlar[a)]
Department of Chemistry and Supercomputing Institute, University of Minnesota, Minneapolis, Minnesota 55455-0431

(Received 29 January 2001; accepted 17 April 2001)

A family of four weakly coupled electronically nonadiabatic bimolecular model photochemical systems is presented. Fully converged quantum mechanical calculations with up to 25 269 basis functions were performed for full-dimensional atom–diatom collisions to determine the accurate scattering dynamics for each of the four systems. The quantum mechanical probabilities for electronically nonadiabatic reaction and for nonreactive electronic deexcitation vary from 10^{-1} to 10^{-5}. Tully's fewest-switches (TFS) semiclassical trajectory surface-hopping method (also called molecular dynamics with quantum transitions or MDQT) is tested against the accurate quantal results. The nonadiabatic reaction and nonreactive deexcitation events are found to be highly classically forbidden for these systems, which were specifically designed to model classically forbidden electronic transitions (also called frustrated hops). The TFS method is shown to systematically overestimate the nonadiabatic transition probabilities due to the high occurrence of frustrated hops. In order to better understand this problem and learn how to best minimize the errors, we test several variants of the TFS method on the four new weakly coupled systems and also on a set of three more strongly coupled model systems that have been presented previously. The methods tested here differ from one another in their treatment of the classical trajectory during and after a frustrated hopping event. During the hopping event we find that using a rotated hopping vector results in the best agreement of semiclassical and quantal results for the nonadiabatic transition probabilities. After the hopping event, we find that ignoring frustrated hops instead of reversing the momentum along the nonadiabatic coupling vector results in the best agreement with the accurate quantum results for the final vibrational and rotational moments. We also test the use of symmetrized probabilities in the equations for the TFS hopping probabilities. These methods systematically lead to increased error for systems with weakly coupled electronic states unless the hopping probabilities are symmetrized according to the electronic state populations. © *2001 American Institute of Physics.* [DOI: 10.1063/1.1377891]

I. INTRODUCTION

Semiclassical methods for calculating the probabilities of electronically nonadiabatic events have a long history,[1] and a variety of multistate approximations have been developed and reviewed.[2–6] An important recent development is the use of converged quantum mechanical dynamics calculations for full-dimensional atom–molecule collisions to test the semiclassical theories.[7–17]

One may classify electronically nonadiabatic systems in various ways, the simplest of which recognizes strongly coupled and weakly coupled systems. The former are epitomized by surface intersections and localized, narrowly avoided crossings, the so-called Landau–Zener–Teller case,[1,2,4,18] and the latter are epitomized by wide regions of coupling, often of weakly coupled but nearly parallel potential functions, the so-called Rosen–Zener–Demkov case.[1,2,4,19,20] The present article is primarily concerned with developing and testing semiclassical methods for atom–molecule collisions in the latter, less studied case. In particular we focus on the trajectory surface hopping[21–36] (TSH) method and specifically on Tully's fewest-switches (TFS) algorithm[6,30] for surface hopping. (TFS is also called molecular dynamics with quantum transitions or MDQT.) Surface hopping is an *ad hoc* addition to classical mechanics in which trajectories instantaneously switch electronic states, i.e., the potential energy function that determines the nuclear motion is discontinuous. The TFS algorithm is an affordable and often accurate method[7–14] despite the apparent shortcoming of using sudden surface switches (hops) to describe the nonadiabatic flow of probability in electronic state space.

There are two important decisions that must be made when implementing surface hopping: (1) When a surface hop to a different electronic state is called for and is classically allowed, how should the kinetic energy be adjusted so as to conserve total energy and (2) what is the best way to treat hopping attempts that are classically forbidden? The first question has a satisfactory answer. The direction along which the nuclear momentum is adjusted is represented by a unit vector called the hopping vector, and it has been shown[9,11] that using the direction of the nonadiabatic coupling vector (instead of the gradient of the electronic energy gap, for example) as the hopping vector and adjusting the

a)Electronic mail: truhlar@umn.edu

nuclear momentum such that total energy is conserved results in the best agreement with quantum mechanical calculations. This procedure has also been justified theoretically.[22,28,37]

Our present study will concentrate on the second question. Hopping attempts that are classically forbidden are called frustrated hops, and their treatment has attracted some attention recently,[12,14,34–36,38,39] but a satisfactory procedure has not yet been obtained. It has been suggested that frustrated hops should be ignored, and this method has been applied with some success.[34] It has also been argued[23,25,38] that when a trajectory experiences a frustrated hop, the nuclear momentum should be reversed along the hopping vector, as if the trajectory experiences a repulsive wall normal to the hopping vector as it attempts and fails to hop to a higher-energy electronic state. In past works,[7,9–15,27] our group has generally followed the procedure used by Blais and Truhlar;[27] this involves a combination of these two approaches, i.e., energetically forbidden frustrated hops are ignored while energetically allowed but momentum forbidden frustrated hops are reflected.

It has been noted[35] that one may distinguish two possible reasons for the occurrence of classically forbidden hopping attempts. The first possible reason is that the trajectory surface hopping algorithm is somehow inadequate and should not be predicting transitions where they cannot occur. This argument is strengthened by studies that show surface hopping methods to be more accurate when frustrated hops are ignored.[34] Motivated by this reasoning, a variant of the TFS method called the MDQT* method has recently been proposed[35,36] that eliminates hopping attempts in classically forbidden regions by using a symmetrized velocity in the equations for the electronic state populations. The second possible reason for frustrated hops is that the trajectory *should* hop to the energetically forbidden state, but classical trajectories are limited by the conservation of total energy, whereas quantum mechanical particles can borrow energy for a finite time according to the uncertainty principle. This idea suggests that the method for adjusting the nuclear kinetic energy during a hopping attempt is somehow deficient. Our group has recently proposed a method for redistributing the nuclear kinetic energy in order to allow some classically forbidden hops,[12,14] although this method generally led to increased semiclassical errors for the cases to which it was applied.

In a recent work,[13] two semiclassical methods were tested against accurate quantum mechanical calculations for the weakly coupled BrH_2 system, which is a reactive Rosen–Zener–Demkov case. The results show that despite difficulty in achieving numerical convergence, the TFS method is more accurate than the semiclassical Ehrenfest method[40,41] for this case. In the present work we test semiclassical methods on a family of four weakly coupled three-atom systems called the YRH systems with features qualitatively similar to the BrH_2 system. The family of systems has members with quantum mechanical nonadiabatic transition probabilities varying from $\sim 10^{-1}$ to $\sim 10^{-5}$, and it was specifically designed to provide a more systematic test of nonadiabatic semiclassical trajectory methods than the previously described BrH_2 system. Using the TFS algorithm we find for the model systems studied here that hopping to the ground state is rare, but once the system is in the ground state, a large percentage (25%–80%) of trajectories experience at least one frustrated hopping attempt. This results in a breakdown of the self-consistency of the TFS algorithm, i.e., the fraction of trajectories in each state does not correspond to the distribution demanded by the fewest-switches algorithm.

Due to the high percentage of trajectories affected by frustrated hops and the low probability of multiple hopping trajectories, the new YRH model systems presented here provide good test cases for studying the treatment of frustrated hops. We use the family of YRH systems along with a previously described[15] set of more strongly coupled model systems, called MXH systems, to explore several variants of the TFS method which differ in their treatment of frustrated hopping. Section II presents the model YRH systems, and Sec. III presents the accurate quantum mechanical dynamics calculations for these systems. Section IV discusses the semiclassical algorithms, and Secs. V and VI present and discuss the results of the semiclassical methods applied to the model YRH and MXH systems.

II. MODEL POTENTIAL ENERGY MATRICES AND SCATTERING CONDITIONS

In order to design a simple and systematic set of test cases for studying the treatment of surface hops without interference from competing effects, a family of model three-body potential energy matrices (PEMs) with weakly coupled electronic states was created. Each PEM models the nonadiabatic scattering process of an electronically excited model Y atom interacting with a diatomic RH molecule initially in some discrete vibrational and rotational quantum state (ν,j):

$$\mathrm{Y}^*+\mathrm{RH}(\nu,j)\rightarrow\begin{cases}\mathrm{Y}+\mathrm{RH}(\nu'',j'') & \text{(R1a)}\\ \mathrm{R}+\mathrm{YH}(\nu',j'), & \text{(R1b)}\end{cases}$$

where the asterisk indicates electronic excitation, and the primes on the quantum numbers indicate that these quantities are not conserved. There is some probability P_R that the system will react to form the YH diatomic product (R1b) and some probability P_Q that the system will quench, typically accompanied by vibrational and rotational excitation of the RH diatom (R1a). The sum of these probabilities is the total nonadiabatic probability P_N for the system to undergo an electronic transition to the ground state during the scattering event.

The electronic excitation energy of the Y atom is taken as 0.36 eV, and the equilibrium bond energies of the RH and YH molecules are 3.9 and 4.3 eV, respectively. The zero point energies of RH and YH are 0.18 and 0.19 eV, respectively. The mass combination for all calculations was chosen to be 10 and 6 amu for the Y and R atoms, respectively. The H atom has the mass of hydrogen, i.e., 1.007 83 amu. This mass combination provides an interesting and challenging test case for semiclassical methods. The system is modeled in the diabatic representation and has qualitative features of the Rosen–Zener–Demkov type,[1,2,19,20] i.e., the diagonal diabatic potential energy surfaces U_{11} and U_{22} never cross and

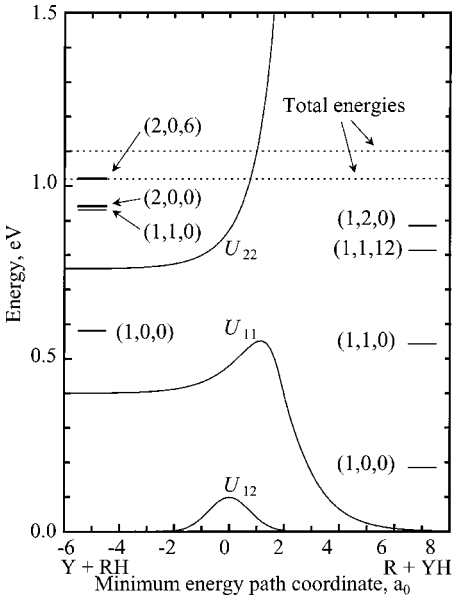

FIG. 1. Values of the diabatic potential energy matrix elements U_{11}, U_{12}, and U_{22} plotted as a function of an approximate reaction coordinate for the ground state reaction Y+RH→R+YH at a fixed YRH bond angle of 120°. The U_{12} curve shown corresponds to the YRH(0.10) PEM. Also shown are the two scattering energies used in this study, as well as the energies of several asymptotic rovibrational states (χ,ν,j), where χ is the electronic quantum number, ν is the vibrational quantum number, and j is the rotational quantum number.

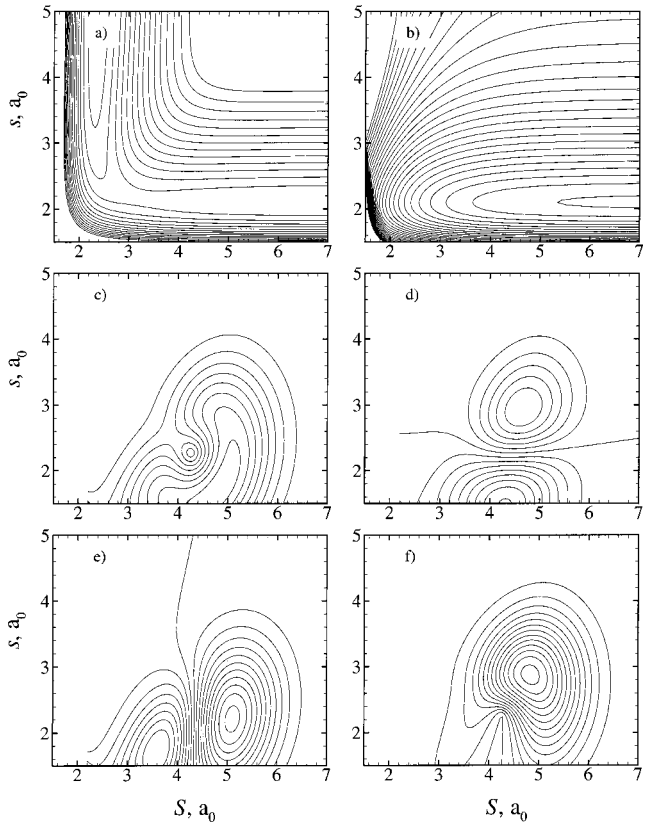

FIG. 2. Contour plots of the adiabatic energies and the nonadiabatic coupling vector, plotted as functions of the translational Jacobi coordinate S, and the diatomic Jacobi coordinate s, with the Jacobi angle $\chi=120°$. (a) Lower-energy adiabatic potential energy surface. (b) Higher-energy adiabatic potential energy surface. (c) Magnitude of the nonadiabatic coupling vector $|\mathbf{d}|$. (d) Magnitude of the component of **d** that lies in the direction of the diatomic Jacobi coordinate. (e) Magnitude of the component of **d** that lies in the direction of the translational Jacobi coordinate. (f) Magnitude of the component of **d** that lies in the direction of the Jacobi angle. For panels (a) and (b), the lowest energy contours are at 0.2 and 0.8 eV, respectively, and the contour spacing is 0.2 eV. For panels (c), (d), and (f) the contour spacing is $10^{-4}a_0^{-1}$. For panel (e) the contour spacing is $10^{-5}a_0^{-1}$.

are nearly parallel in the entrance valley. The diabatic coupling U_{12} is localized in the interaction region. The energy gap between the diabatic surfaces is roughly equal to 0.36 eV throughout the strong interaction region. Details of the functional forms and the parameters used in the analytic representation of the family of YRH surfaces are available as supporting information.[42]

Each member of the family of YRH matrices differs from the others only in the value of the maximum diabatic coupling $U_{12}^{\max}$. Four potential matrices with values of $U_{12}^{\max}=0.20$, 0.10, 0.03, and 0.01 eV are discussed in this paper. The PEMs in the series will be referred to individually as YRH($U_{12}^{\max}$/eV), where $U_{12}^{\max}$/eV is $U_{12}^{\max}$ in eV, e.g., YRH(0.20). A plot of the diabatic matrix elements U_{11}, U_{12}, and U_{22} along an approximate reaction path of U_{11} in the internuclear bond distance coordinate system is given for YRH(0.10) in Fig. 1. Also shown in Fig. 1 are the two different total scattering energies (1.10 and 1.02 eV) used for the calculations reported in this paper and the energies of some asymptotic rovibrational states.

Adiabatic potential energy surfaces were obtained by diagonalizing the diabatic PEM. In the adiabatic representation the scalar product of the velocity and the nonadiabatic coupling vector **d** (due to the nuclear linear momentum) couples the nuclear and electronic degrees of freedom.[6,24] Using the Hellman–Feynman theorem, we can calculate **d** without approximation from the diabatic matrix elements and their gradients.[24] Figure 2 contains contour plots of the upper and lower adiabatic surfaces and the magnitude of **d**. Also shown are the magnitudes of the three components of **d**, expressed in the reactant-Jacobi coordinate system, where S is the magnitude of the vector **S** that points from Y to the center-of-mass of RH, s is the magnitude of the vector **s** that points from R to H, and χ is the angle between **S** and **s**.

Initial scattering conditions may be labeled by the shorthand $(E/\text{eV},j)$ where E/eV is the total energy in eV and j is the initial rotational quantum number; in all cases the initial electronic quantum number is 2 (which corresponds to the excited electronic state), the initial vibrational quantum number is 0, and the total angular momentum is 0. We consider three cases for the YRH systems: (1.10, 0), (1.10, 6), and (1.02, 0). Note that the initial total internal energy for a collision of Y* with RH($\nu=0,j=0$) is 0.94 eV and that for RH($\nu=0,j=6$) is 1.02 eV.

Although this paper focuses on the model YRH systems, we also consider the previously described[15] set of MXH model PEMs. These systems are more strongly coupled than the YRH systems; the quantum mechanical nonadiabatic transition probabilities vary from 0.15 to 0.49. For these systems we consider the $(m_{\mathrm{M}},m_{\mathrm{X}},m_{\mathrm{H}})=(6.046\,95,2.015\,65,1.007\,83\,\text{amu})$ mass combination and the (1.10, 0) set of initial conditions. We consider all three

sets of MXH surfaces which were previously[15] labeled SB, SL, and WL. See Ref. 15 for a complete description of the MXH surfaces.

III. QUANTUM DYNAMICS FOR THE MODEL YRH SYSTEMS

Fully converged, six-dimensional (three vibrations and three rotations) quantum mechanical scattering calculations were performed on each of the four YRH potential energy matrices using the outgoing wave variational principle (OWVP),[43–46] as implemented in version 18.8 of the VP computer code.[47] The OWVP is a linear algebraic variational principle[48] employing both $\mathcal{L}^2$ and non-$\mathcal{L}^2$ basis functions. The calculations reported here employ a basis of asymptotic eigenstate functions multiplied by half-integrated Green's functions[49] for energetically open channels and by Gaussian functions for energetically closed channels. A channel is defined as a unique set of the asymptotic quantum numbers including: the molecular arrangement, the diabatic electronic quantum number, the vibrational quantum number of the diatomic molecule, and the rotational quantum number of the diatomic molecule. (For nonzero total angular momentum J one could also include the relative translational orbital angular momentum ℓ, but for $J=0$, we have ℓ equal to j, j', or j''.) All of the rotational-state channels for a given vibrational state, electronic state, and molecular arrangement were coupled to each other, whereas channels with different vibrational states, electronic states, or molecular arrangements were uncoupled when solving the finite difference problem to obtain the basis functions for the variational step. The surfaces were fully coupled during the variational step of the calculations. See Refs. 43–46 for details.

We define our potential energy matrices and perform our quantum mechanical calculations in the diabatic representation with zero nuclear momentum coupling. In such a model, there is a one-to-one transformation between diabatic and adiabatic representations, and the quantum mechanical results are independent of which one is chosen.

A list of the OWVP basis set parameters can be found in the supporting information.[42] Basis set I contains 18 934 basis functions and was used to calculate all of the observables reported in this paper. The larger basis set, basis set II was used to check the convergence of basis set I for the YRH(0.20) and YRH(0.01) systems at several scattering energies. The number of basis functions in the convergence check is 25 269. In these convergence checks, the state-to-state transition probabilities out of the $Y^*+RH(\nu=0,j=0)$ (for $E=1.10$ and 1.02 eV) and the $Y^*+RH(\nu=0,j=6)$ (for $E=1.10$ eV) initial states are converged to better than 1% for greater than 95% of the energetically accessible final channels, with the remaining state-to-state transition probabilities (high-j' or j'' channels) converged to better than 5%. For all of the state-to-state transition probabilities (including all initial states), 94% of the transition probabilities (with an average value of 0.013) are converged to better then 1%, 3% of the transition probabilities (with an average value of 4.5×10^{-5}) are converged to better than 5%, and the remaining 3% of the transition probabilities have an average value of 2.1×10^{-8}. The first moments (i.e., averages) of the vibrational and rotational quantum numbers and the reaction and quenching probabilities are converged to better than 1%.

Quantum mechanical observables often exhibit an oscillatory structure as functions of scattering energy. In contrast, semiclassical properties often do not show these oscillations, and in such cases it is most appropriate to compare them to energy-averaged quantum results. In the present case we checked that the semiclassical results depend only slowly on energy. It is therefore desirable to compare the semiclassical results obtained at a single scattering energy to the average quantum mechanical value obtained over a range of energies. Quantum mechanical calculations were performed at seven energies at and around the nominal scattering energies[42] and averaged to obtain values that are used to compute the errors reported in Tables II and III. In most cases, the values obtained by averaging are similar to the values obtained at the nominal scattering energy.

IV. SEMICLASSICAL TRAJECTORY CALCULATIONS

Semiclassical trajectory surface hopping calculations were carried out using version 6.0 of the NAT computer code[50] (which is a generalized version of our previous TSH code). For all the calculations reported in this work, the hopping vector was taken to be a unit vector in the direction of the nonadiabatic coupling vector, i.e.,

$$\mathbf{h}=\frac{\mathbf{d}}{|\mathbf{d}|}. \tag{1}$$

The initial coordinates and momenta for each trajectory in the ensemble were selected as described previously.[11,25]

The final reaction and quenching probabilities (P_R and P_Q) were determined by counting trajectories, and the final rotational and vibrational moments ($\langle v'\rangle$ and $\langle j'\rangle$ for reactive trajectories, and $\langle v''\rangle$ and $\langle j''\rangle$ for quenching trajectories) were calculated according to the energy-nonconserving histogram (ENH) analysis scheme.[11] Vibrational and rotational moments were also calculated using the energy-nonconserving quadratic smooth sampling[11,51] (ENQSS), and the energy-nonconserving linear smooth sampling (ENLSS) analysis schemes. We also tested an energy-conserving (EC) variant[11] of the three sampling schemes, i.e., ECH, ECQSS, and ECLSS. The EC methods result in systematically slightly lower rotational and vibrational moments and lead to increased semiclassical errors. The results from the six analysis schemes typically differ from each other by less than 2%. For this reason we report only one set of results, and we chose the ENH result, because it has a well-defined statistical uncertainty estimate.[25]

IV.A. Treatment of the nuclear momentum at a frustrated hop

During a surface hopping event, a trajectory attempts to hop from the occupied electronic state to a target electronic state. A hopping attempt is classically forbidden if it is not possible to adjust the nuclear momenta along the hopping vector **h**, such that total energy is conserved. One may further divide classically forbidden hops into three categories,[12] namely: energy-, angular-momentum-, and linear-momentum-forbidden hops. Energy-forbidden hops occur

when the target state has an energy greater than the total energy of the system. The distinction between the other two types of frustrated hops depends on dividing the energy into vibrational and rotational contributions. A hop is angular-momentum-forbidden when the hop is not energy-forbidden, but the vibrational energy is less than the energy of the target state, i.e., the nuclear momentum cannot be adjusted in any direction such that total angular momentum is conserved. A linear-momentum-forbidden hop occurs when there is sufficient energy in vibrational modes to exist on the target surface, but there is insufficient energy along the hopping vector **h** to allow for the energy adjustment. We note that for systems where the total angular momentum J is equal to zero, there is no energy in the rotation of the system and angular-momentum-forbidden hops cannot occur. For the calculations reported here, the orbital angular momentum ℓ_{class} is selected classically from $0 \leqslant \ell_{\text{class}} \leqslant \hbar$ for the $j=0$ state and from $6\hbar \leqslant \ell_{\text{class}} \leqslant 7\hbar$ for the $j=6$ state, and therefore the total angular momentum J can have values that range from $-\frac{1}{2}\hbar < J < \frac{1}{2}\hbar$. The occurrence of angular-momentum-forbidden hops, however, is much less than 0.01% of the total number of attempted hops, and the treatment of angular-momentum-forbidden (but otherwise allowed) hops will not be considered in this paper.

Several variants of the TFS method which differ in their treatment of frustrated hops will be tested. We will refer to the TFS variants as TFS-(Prot-L, Prot-E), where Prot-L denotes the protocol for linear-momentum-forbidden hops, and Prot-E denotes the protocol for energy-forbidden hops. The allowed values for Prot-L and Prot-E will be introduced and defined as needed.

In recent work,[7,9–15] following an older protocol,[27] our group has used an implementation of the TFS method in which momentum- and energy-forbidden hops are treated differently. When a trajectory experiences a linear-momentum-forbidden hop, the nuclear momentum along the hopping vector **h** is reversed, whereas when a trajectory experiences an energy-forbidden hop, the attempted hop is ignored. We will refer to this method as the TFS-(−,+) method, where the "−" indicates that the nuclear momentum is reversed along **h**, and the "+" indicates that the nuclear momentum is not reversed along **h**. In assessing whether this is the best procedure, we note that interstate coupling in the adiabatic representation is proportional to the scalar product of the velocity of the trajectory and **d**, and therefore it is independent of the components of the velocity orthogonal to **d**. We also note that it is the energy in the modes orthogonal to **d** that differentiates the two different types of forbidden hops. These considerations motivate a method that treats frustrated hops consistently. In particular, along with the TFS-(−,+) method, we test two alternate schemes, namely the TFS-(+,+) and the TFS-(−,−) methods. In the TFS-(−,−) method, all frustrated hops are reflected along **h**. The TFS-(−,−) method was the method used in the original implementation of the TFS method.[30,38] In the TFS-(+, +) method, all frustrated hops are ignored. The TFS-(+, +) method has also been suggested and tested in the literature.[34]

We have previously described a method for removing linear-momentum-frustrated hops by rotating the hopping vector **h** within the zero angular momentum region of configuration space by the smallest amount that allows for hopping.[12] In the present work we call this the TFS-(R, +) method, where the "R" indicates that linear-momentum-forbidden hops are allowed using a rotated hopping vector. Rotating the hopping vector cannot be used to allow energy-forbidden hops, and when an energy-forbidden hop is attempted, it is ignored.

IV.B. Symmetrized-speed and symmetrized-coupling methods

The four variants of the TFS method discussed in the previous section, TFS-(−,+), TFS-(−,−), TFS-(+,+), and TFS-(R,+), differ in their treatment of the classical trajectory after a hopping attempt that is generated by the TFS algorithm turns out to be frustrated. An alternate approach is to modify the TFS algorithm to eliminate hopping attempts in regions where hops are classically forbidden. For a trajectory is following the path $\mathbf{R}(t)$, we can write the electronic wave function for a two-state system as

$$\Psi(t) = c_1(t)\phi_1[\mathbf{R}(t)] + c_2(t)\phi_2[\mathbf{R}(t)], \tag{2}$$

where ϕ_1 and ϕ_2 are the adiabatic electronic basis functions for the ground state and excited state, respectively, and c_1 and c_2 are expansion coefficients that depend on the time t. The electronic state population of state χ at time t is given by

$$n_\chi(t) = |c_\chi(t)|^2. \tag{3}$$

The TFS probability of hopping from the occupied electronic state k to the target state l is given by[30]

$$g_{kl} = \max\left(0, \frac{b_{kl}\Delta t}{n_k}\right), \tag{4}$$

where

$$b_{kl} = -2\,\mathrm{Re}(a_{kl}^* \dot{\mathbf{R}}_k \cdot \mathbf{d}), \tag{5}$$

Δt is the change in time between hopping checks, a_{kl} is the electronic state coherence $c_k c_l^*$, and $\dot{\mathbf{R}}_k$ is the velocity of the system on the occupied surface k. When a hop occurs, the internal energy is adjusted along the **h** vector, such that energy is conserved, i.e., according to the following equation

$$T_{\mathbf{h}}(k) + E(k) = T_{\mathbf{h}}(l) + E(l), \tag{6}$$

where $T_{\mathbf{h}}(k)$ is the kinetic energy associated with the component of the nuclear linear momentum in the **h** direction when the trajectory is on surface k, and $E(k)$ is the potential energy of surface k. As mentioned previously, a hopping attempt is frustrated if the energy of the occupied state k is less than the energy of the target state l, and the kinetic energy along **h** before the hopping attempt is less than the energy gap between the two potential energy surfaces, i.e., if

$$T_{\mathbf{h}}(k) < E(l) - E(k). \tag{7}$$

A method called the MDQT* method[35,36] has been proposed for the case where Eq. (4) is used, such that one uses a geometrically symmetrized speed (GS) to eliminate hopping attempts in regions where Eq. (7) is true. This method

was justified[35] by noting that while a TFS classical trajectory exists on only one potential energy surface, a quantum mechanical wave function has some probability density on both electronic surfaces, and hence the magnitude of the velocity that appears in the electronic dynamics through Eq. (5) is replaced by a speed more representative of the motion on both surfaces. We test this method along with seven variants. All eight methods eliminate frustrated hopping by rewriting Eq. (5) as

$$b'_{kl} = -2\,\mathrm{Re}[a^*_{kl} F(\dot{\mathbf{R}}_k, \dot{\mathbf{R}}_l, \mathbf{d})], \tag{8}$$

where the exact form of $F(\dot{\mathbf{R}}_k, \dot{\mathbf{R}}_l, \mathbf{d})$ depends on the method. (Note that a_{kl} is also a function of $\dot{\mathbf{R}}_k \cdot \mathbf{d}$, and $F(\dot{\mathbf{R}}_k, \dot{\mathbf{R}}_l, \mathbf{d})$ is used in place of $\dot{\mathbf{R}}_k \cdot \mathbf{d}$ when calculating a_{kl} for the eight new methods presented here.) In the MDQT* method, which we will also call the GS(1/2) method,

$$F^{\mathrm{GS}(1/2)}(\dot{\mathbf{R}}_k, \dot{\mathbf{R}}_l, \mathbf{d}) = |\dot{\mathbf{R}}_k|^{1/2} |\dot{\mathbf{R}}_l|^{1/2} \frac{\dot{\mathbf{R}}_k \cdot \mathbf{d}}{|\dot{\mathbf{R}}_k|}, \tag{9}$$

where the velocity of the trajectory in the currently occupied electronic state is $\dot{\mathbf{R}}_k$. The value of $|\dot{\mathbf{R}}_l|$ must be computed at each time step, where $\dot{\mathbf{R}}_l$ is the velocity that the trajectory would have if it were to hop to the other electronic surface. Whenever a hopping attempt would be frustrated, $\dot{\mathbf{R}}_l$ does not exist, and $F(\dot{\mathbf{R}}_k, \dot{\mathbf{R}}_l, \mathbf{d})$ is set to zero. All frustrated hops are eliminated in this method. The hopping probability does not go smoothly to zero as hopping becomes frustrated because $\dot{\mathbf{R}}_l$ can have nonzero components orthogonal to $\mathbf{d}$ as hopping becomes frustrated.

We also note that in the GS(1/2) method,[35,36] the components of the velocity orthogonal to $\mathbf{d}$ contribute to the electronic dynamics. This might be considered unphysical since, as previously mentioned, these components do not couple the adiabatic electronic states in the original equation for b_{kl} given in Eq. (5). An alternate prescription that eliminates frustrated hopping with a smoothly vanishing hopping probability function is the geometrically symmetrized coupling scheme, GC(1/2). In this formulation,

$$F^{\mathrm{GC}(1/2)}(\dot{\mathbf{R}}_k, \dot{\mathbf{R}}_l, \mathbf{d}) = |\dot{\mathbf{R}}_k \cdot \mathbf{d}|^{1/2} |\dot{\mathbf{R}}_l \cdot \mathbf{d}|^{1/2} \frac{\dot{\mathbf{R}}_k \cdot \mathbf{d}}{|\dot{\mathbf{R}}_k \cdot \mathbf{d}|}. \tag{10}$$

Using Eq. (10), the hopping probability goes smoothly to zero as hopping becomes frustrated. The GC(1/2) method symmetrizes only the component of the velocity which is along $\mathbf{d}$; the components of the velocity orthogonal to $\mathbf{d}$ do not contribute to the electronic dynamics, which is consistent with Eq. (5).

For completeness we also test the AS(1/2) and AC(1/2) methods, in which the speed or the coupling is arithmetically symmetrized. Specifically,

$$F^{\mathrm{AS}(1/2)}(\dot{\mathbf{R}}_k, \dot{\mathbf{R}}_l, \mathbf{d}) = (\tfrac{1}{2}|\dot{\mathbf{R}}_k| + \tfrac{1}{2}|\dot{\mathbf{R}}_l|) \frac{\dot{\mathbf{R}}_k \cdot \mathbf{d}}{|\dot{\mathbf{R}}_k|}, \tag{11}$$

$$F^{\mathrm{AC}(1/2)}(\dot{\mathbf{R}}_k, \dot{\mathbf{R}}_l, \mathbf{d}) = (\tfrac{1}{2}|\dot{\mathbf{R}}_k \cdot \mathbf{d}| + \tfrac{1}{2}|\dot{\mathbf{R}}_l \cdot \mathbf{d}|) \frac{\dot{\mathbf{R}}_k \cdot \mathbf{d}}{|\dot{\mathbf{R}}_k \cdot \mathbf{d}|}. \tag{12}$$

The symmetrized coupling equations for the GS(1/2), GC(1/2), AS(1/2), and AC(1/2) methods defined in Eqs. (9)–(12) weight the speed or coupling of both surfaces equally. In general, the wave packet is not evenly distributed between the two electronic states. In order to incorporate this into the dynamics we define the method GC(n_χ) by rewriting Eq. (10) as

$$F^{\mathrm{GC}(n_\chi)}(\dot{\mathbf{R}}_k, \dot{\mathbf{R}}_l, \mathbf{d}) = |\dot{\mathbf{R}}_k \cdot \mathbf{d}|^{n_k} |\dot{\mathbf{R}}_l \cdot \mathbf{d}|^{n_l} \frac{\dot{\mathbf{R}}_k \cdot \mathbf{d}}{|\dot{\mathbf{R}}_k \cdot \mathbf{d}|}, \tag{13}$$

where n_χ is the electronic state population of state χ. With this form of $F^{\mathrm{GC}(n_\chi)}$, the coupling terms that arise from each electronic surface are weighted according to their state populations n_χ instead of arbitrarily by $\frac{1}{2}$. We also test the GS(n_χ), AS(n_χ), and AC(n_χ) methods which are defined by replacing the $\frac{1}{2}$ weighting factors that appear in Eqs. (9), (11), and (12), respectively, by n_χ, specifically:

$$F^{\mathrm{GS}(n_\chi)}(\dot{\mathbf{R}}_k, \dot{\mathbf{R}}_l, \mathbf{d}) = |\dot{\mathbf{R}}_k|^{n_k} |\dot{\mathbf{R}}_l|^{n_l} \frac{\dot{\mathbf{R}}_k \cdot \mathbf{d}}{|\dot{\mathbf{R}}_k|}, \tag{14}$$

$$F^{\mathrm{AS}(n_\chi)}(\dot{\mathbf{R}}_k, \dot{\mathbf{R}}_l, \mathbf{d}) = (n_k|\dot{\mathbf{R}}_k| + n_l|\dot{\mathbf{R}}_l|) \frac{\dot{\mathbf{R}}_k \cdot \mathbf{d}}{|\dot{\mathbf{R}}_k|}, \tag{15}$$

$$F^{\mathrm{AC}(n_\chi)}(\dot{\mathbf{R}}_k, \dot{\mathbf{R}}_l, \mathbf{d}) = (n_k|\dot{\mathbf{R}}_k \cdot \mathbf{d}| + n_l|\dot{\mathbf{R}}_l \cdot \mathbf{d}|) \frac{\dot{\mathbf{R}}_k \cdot \mathbf{d}}{|\dot{\mathbf{R}}_k \cdot \mathbf{d}|}. \tag{16}$$

IV.C. Absorbing frustrated hops

It is interesting to calculate the reaction and quenching probabilities that would be obtained by the TFS method if somehow frustrated trajectories were provided with the necessary energy to hop. We can obtain a lower limit on the total nonadiabatic probability P_N by reanalyzing the data from a TFS calculation and using only those trajectories that do not experience a frustrated hop to calculate the final probabilities and moments. This method can be thought of as the result obtained by absorbing trajectories with frustrated hops to the upper electronic state and is called the AFH result. This result provides a lower limit on the TFS total nonadiabatic probability P_N because the possibility that some of the reassigned trajectories may hop back down to the lower state is not included. Note that the TFS-AFH method cannot be used to compute the moments on the upper surface, but we do not consider such moments in the present paper.

IV.D. Semiclassical Ehrenfest method

Although our main goal here is to determine the optimum procedure for trajectory surface hopping calculations when the surfaces are weakly coupled, we also carried out calculations using the semiclassical Ehrenfest version[39,40] of the time-dependent self-consistent-field method. The calcula-

TABLE I. Reaction, quenching, and total nonadiabatic transition probabilities, final vibrational and rotational moments, and product branching ratios for the YRH(0.20) system and the (1.10, 0) initial conditions.

Method	P_R	$\langle \nu' \rangle$	$\langle j' \rangle$	P_Q	$\langle \nu'' \rangle$	$\langle j'' \rangle$	F_R	P_N
Quantum[a]	0.010	0.83	12.4	0.047	0.90	3.35	0.176	0.057
Average quantum[b]	0.012	0.93	12.1	0.045	0.90	3.30	0.213	0.057
TFS-(−,+)	0.034	0.77	13.1	0.068	0.47	5.57	0.333	0.102
TFS-AFH	0.007	0.81	13.9	0.020	0.35	7.92	0.256	0.027
TFS-(+,+)	0.035	0.90	12.7	0.066	0.65	5.12	0.349	0.101
TFS-(−,−)	0.027	0.81	12.7	0.073	0.45	5.77	0.272	0.101
TFS-(R,+)	0.020	0.84	13.5	0.035	0.56	5.95	0.361	0.055
GS(1/2)≡MDQT*	0.057	0.85	13.1	0.109	0.62	5.67	0.342	0.166
GC(1/2)	0.097	0.95	12.3	0.165	0.66	5.41	0.369	0.262
AS(1/2)	0.133	0.97	12.2	0.234	0.66	5.22	0.362	0.367
AC(1/2)	0.062	0.86	13.0	0.116	0.65	5.14	0.349	0.178
GS(n_χ)	0.038	0.87	12.8	0.067	0.62	5.74	0.359	0.105
GC(n_χ)	0.040	0.89	12.8	0.075	0.63	5.61	0.346	0.115
AS(n_χ)	0.040	0.86	12.9	0.070	0.59	6.03	0.364	0.110
AC(n_χ)	0.035	0.85	13.0	0.063	0.59	5.90	0.360	0.098
TFS-(−,+)-di	0.331	0.54	12.5	0.269	0.40	5.50	0.552	0.600
TFS-AFH-di	0.001	1.00	14.0	0.015	0.14	5.26	0.075	0.016

[a]Quantum mechanical result for the scattering energy 1.10 eV.
[b]Average of seven quantum mechanical calculations performed at the following scattering energies: 1.07, 1.08, 1.09, 1.10, 1.11, 1.12, and 1.13 eV.

tions show that the Ehrenfest method fails badly for these systems, and this finding further motivates the present study. The Ehrenfest results are discussed briefly in the appendix.

V. RESULTS

We tested all of the methods mentioned in this paper on the YRH(0.2) PEM at the (1.10, 0) set of initial conditions, and the results are summarized in Table I. We further tested the TFS-(−, +), TFS-(+, +), TFS-(−, −), TFS-(R, +), and GC(n_χ) methods on all four of the YRH PEMs at each of the three different sets of initial conditions (1.10, 0), (1.10, 6), and (1.02, 0) and on the set of three model MXH systems (SB, SL, and WL) for the (1.10, 0) set of initial conditions. The detailed results of all of the semiclassical trajectory calculations can be found in the supporting information.[42]

Unless one single semiclassical method is best for all observables for all cases, the choice of ''best method'' is not unique. Nevertheless, we will present some statistics that will help us to determine a reasonable (if not unique) answer to the question of which method is the most accurate and to quantitatively compare the overall accuracy of several semiclassical methods. First, unsigned errors were computed for each vibrational and rotational moment. The quenching probabilities, reaction probabilities, and total nonadiabatic probabilities vary by several orders of magnitude over the four YRH PEMs, and therefore the errors in these quantities were calculated using logarithms, in particular the unsigned logarithmic error in $\log_{10} P_X$ is given by

$$UE(\log_{10} P_X) = |\log_{10} P_X^{\text{semiclassical}} - \log_{10} P_X^{\text{quantal}}|, \qquad (17)$$

where $X =$ ''R,'' ''Q,'' or ''N.'' We also consider the error in the reactive branching ratio F_R which is defined as the ratio of the reaction probability P_R to the total nonadiabatic probability P_N. The unsigned errors for all of the semiclassical methods discussed in this paper for the YRH(0.20) PEM and the (1.10, 0) set of initial conditions are shown in Table II.

TABLE II. Unsigned errors in the semiclassical methods for the YRH(0.20) system and the (1.10, 0) initial conditions.[a]

Method	$\log_{10} P_R$	$\langle \nu' \rangle$	$\langle j' \rangle$	$\log_{10} P_Q$	$\langle \nu'' \rangle$	(j'')	F_R	$\log_{10} P_N$	Overall[b]
TFS-(−,+)	0.45	0.16	0.99	0.18	0.43	2.27	0.12	0.25	0.62
TFS-(+,+)	0.46	**0.04**	0.66	0.16	**0.25**	**1.81**	0.14	0.24	**0.44**
TFS-(−,−)	0.35	0.12	0.61	0.21	0.45	2.47	**0.06**	0.24	0.52
TFS-(R,+)	**0.21**	0.10	1.44	**0.11**	0.34	2.64	0.15	**0.02**	0.54
GS(1/2)≡MDQT*	0.67	0.08	1.01	0.38	0.28	2.37	0.13	0.46	0.64
GC(1/2)	0.90	**0.01**	**0.22**	0.56	**0.24**	2.11	0.16	0.66	0.61
AS(1/2)	0.71	0.08	0.95	0.41	**0.25**	**1.84**	0.14	0.49	0.64
AC(1/2)	1.04	**0.03**	**0.07**	0.71	**0.24**	**1.91**	0.15	0.81	0.68
GS(n_χ)	0.49	0.06	0.71	0.17	0.28	2.44	0.15	0.26	0.50
GC(n_χ)	0.51	0.05	0.75	0.22	0.27	2.30	0.13	0.30	0.50
AS(n_χ)	0.46	0.08	0.87	0.14	0.31	2.60	0.15	0.23	0.53
AC(n_χ)	0.52	0.07	0.81	0.19	0.31	2.73	0.15	0.28	0.55
TFS-(−,+)-di	1.43	0.40	0.40	0.77	0.50	2.20	0.34	1.02	1.28

[a]Numbers in bold indicate the method with the lowest error for each column. See text for a complete discussion.
[b]To obtain the overall mean error, each column was normalized to have a mean value of 0.62, which is the average value of all unsigned errors in the table. Then the eight columns for a given method were averaged.

TABLE III. Mean unsigned errors in the semiclassical methods averaged over 12 YRH cases and three MXH cases.[a]

System	Method	$\log_{10}P_R$	$\langle\nu'\rangle$	$\langle j'\rangle$	$\log_{10}P_Q$	$\langle\nu''\rangle$	$\langle j''\rangle$	F_R	$\log_{10}P_N$	Overall[b]
YRH[c]	TFS-(−,+)	0.36	0.25	**1.4**	**0.11**	0.36	2.2	0.11	0.13	0.59
	TFS-(+,+)	0.36	**0.15**	**1.3**	**0.10**	**0.22**	**1.9**	0.11	0.11	**0.47**
	TFS-(−,−)	**0.29**	0.25	**1.4**	**0.13**	0.38	2.2	**0.07**	0.13	**0.58**
	TFS-(R,+)	**0.30**	**0.15**	**1.5**	**0.13**	**0.25**	**2.1**	0.13	**0.09**	**0.51**
	GC(n_χ)	0.37	**0.18**	**1.5**	**0.13**	**0.23**	**2.1**	0.11	0.15	**0.54**
MXH[d]	TFS-(−,+)	0.37	**0.06**	**1.2**	0.09	**0.06**	0.43	0.23	0.16	**0.37**
	TFS-(+,+)	0.37	**0.07**	**1.1**	**0.06**	**0.06**	0.39	0.23	0.16	**0.35**
	TFS-(−,−)	0.32	**0.08**	**1.3**	0.10	**0.07**	0.50	**0.18**	0.15	0.36
	TFS-(R,+)	0.37	**0.06**	1.3	0.16	**0.05**	0.60	0.27	**0.12**	0.42
	GC(n_χ)	0.37	**0.07**	**1.2**	0.13	**0.06**	**0.27**	0.20	0.20	**0.40**

[a]Numbers in bold indicate the method with the lowest error for each column. See text for a complete discussion.
[b]To obtain the overall mean error, each column was normalized to have a mean value of 0.46, which is the average value of all unsigned errors in the table. Then the eight columns for a given method were averaged.
[c]Average of the 12 unsigned errors from all four YRH PEMs (0.20, 0.10, 0.03, and 0.01) at all three sets of initial conditions.
[d]Average unsigned error from the three MXH PEMs (SB, SL, and WL) at the (1.10, 0) set of initial conditions.

The method with the lowest unsigned error is listed in bold. If another semiclassical method has an uncertainty that overlaps that of the best method, that method is also listed in bold.

Mean unsigned errors (MUEs) were calculated for the TFS-(−, +), TFS-(+, +), TFS-(−, −), TFS-(R, +), and GC(n_χ) semiclassical methods for the YRH systems by averaging over the 12 cases studied here (four YRH PEMs and three sets of initial conditions) and are presented in Table III. Table IV shows the MUEs for five semiclassical methods for the MXH systems, averaged over the three MXH PEMs. In each column, the method with the smallest MUE is indicated with bold font. By adding and subtracting the uncertainty of the observable from the nominal values, we obtain an upper and a lower bound on the value of the observables. We can then compute an upper bound on the MUEs by calculating the MUE using either the upper or lower value of each observable, whichever results in the greatest error. A lower bound on the MUE can be calculated in a similar way. Taken together, these values were used to determine if the method with the lowest MUE is statistically different from the other methods. If the method with the lowest MUE has an uncertainty in its MUE that overlaps with the uncertainty in the MUE of one or more of the other methods, then each method with overlapping MUEs is also listed in bold in Table III.

Table IV evaluates the semiclassical methods in a different way; in particular, it presents ''scorecards'' for the five semiclassical methods that we applied to all 15 cases. For each of the observables, a point is given to the method with the lowest absolute error (or absolute error of the logarithms for the probabilities) for each PEM and set of initial conditions. If the best method has an error with an uncertainty that overlaps one or more of the other semiclassical methods, each of the winning methods receives a point. Table V summarizes the data in Tables III and IV.

VI. DISCUSSION

The term ''classically forbidden'' can have a variety of meanings in a technical sense, but it is nevertheless useful and easily understood as a label for certain kinds of events. Consider, e.g., the expansion of the electronic wave function Ψ given in Eq. (2). At the start of the simulation, the system is in a pure state, i.e., $c_\chi(t=0)$ is a Kronecker delta, $\delta_{\chi 2}$. It would be reasonable to say that a hop down is classically forbidden whenever $|c_1(t=\infty)|^2$ is less than $\frac{1}{2}$. With this

TABLE IV. Scorecard for the semiclassical methods summed over 12 YRH cases (four potential energy matrices and three sets of initial conditions) and three MHX cases (three potential energy matrices and one set of initial conditions).

System	Method	$\log_{10}P_R$	$\langle\nu'\rangle$	$\langle j'\rangle$	$\log_{10}P_Q$	$\langle\nu''\rangle$	$\langle j''\rangle$	F_R	$\log_{10}P_N$	Probabilities[a]	Moments[b]
YRH[c]	TFS-(−,+)	3	4	7	6	1	2	2	4	15	14
	TFS-(+,+)	1	**9**	**11**	6	**8**	**8**	0	7	14	**36**
	TFS-(−,−)	5	4	8	2	0	3	**9**	6	22	15
	TFS-(R,+)	**9**	**9**	7	**8**	5	5	0	**8**	**25**	26
	GC(n_χ)	3	**9**	8	5	5	3	3	4	15	25
MXH[d]	TFS-(−,+)	0	**3**	**2**	0	1	1	0	0	0	**7**
	TFS-(+,+)	0	2	**2**	**2**	**2**	1	0	0	2	**7**
	TFS-(−,−)	**2**	2	1	0	1	0	**2**	0	**4**	4
	TFS-(R,+)	0	**3**	0	0	1	0	0	**3**	3	4
	GC(n_χ)	1	2	1	1	1	**3**	**2**	0	**4**	**7**

[a]Sum of the four probabilities columns.
[b]Sum of four moments columns.
[c]Twelve cases: four YRH PEMs (0.20, 0.10, 0.03, and 0.01) at three sets of initial conditions.
[d]Three cases: MXH PEMs (SB, SL, and WL) at the (1.10, 0) set of initial conditions.

TABLE V. Overall summary including both YRH and MXH systems.

	Points[a]	Normalized mean unsigned error[b]
Probabilities		
TFS-(−,+)	3.8	0.46
TFS-(+,+)	5.5	0.43
TFS-(−,−)	9.5	0.42
TFS-(R,+)	9.2	0.48
GC(n_χ)	7.8	0.51
Moments		
TFS-(−,+)	10.5	0.50
TFS-(+,+)	16.0	0.39
TFS-(−,−)	7.8	0.52
TFS-(R,+)	10.5	0.45
GC(n_χ)	13.2	0.43
Probabilities and moments		
TFS-(−,+)	14.3	0.48
TFS-(+,+)	21.5	0.41
TFS-(−,−)	17.3	0.47
TFS-(R,+)	19.7	0.46
GC(n_χ)	21.0	0.47

[a]From Table IV with YRH and MXH weighted equally, specifically: $\frac{1}{4}$ YRH points + MXH points.

[b]First, each column in Table III was normalized to have an average value of 0.46. Averages were then computed over the four probabilities, the four moments, or all eight observables with the YRH and MXH surfaces weighted equally.

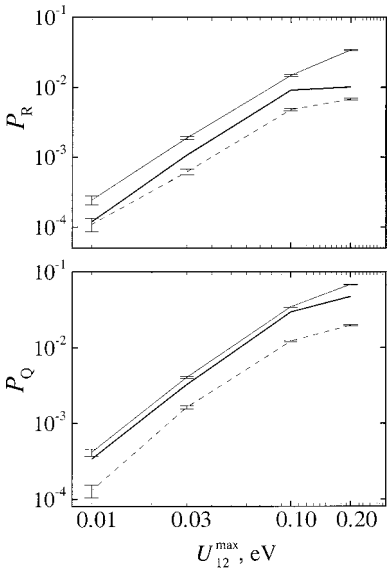

FIG. 3. Reaction and quenching probabilities for the four YRH PEMs and for the initial conditions (1.10, 0). The thick line represents the accurate quantum mechanical results. The solid line with symbols and error bars represents the TFS-(−,+) result. The dashed line with symbols and error bars represents the TFS-AFH result, i.e., the results for absorbing frustrated hops onto the upper surface. Note that both axes are logarithmic.

definition, electronic transitions are classically forbidden for nearly every one of the more than 12 mil trajectories calculated for the YRH systems in the present study. In fact, less than 0.1% of trajectories for YRH(0.20) and YRH(0.10) have values of $|c_1(t=\infty)|^2 > \frac{1}{2}$, and the maximum value of $|c_1(t=\infty)|^2$ is 0.12 and 0.10 for YRH(0.03) and YRH(0.01), respectively. One may therefore expect semiclassical methods to fail for systems with weakly coupled electronic states. We find, however, that the semiclassical methods tested here provide reasonably accurate results, although the results are somewhat sensitive to the treatment of frustrated hops.

The weakly coupled nature of the electronic states of the YRH PEMs requires a large number of trajectories in order to generate good statistics. The number of trajectories computed for each simulation is included in the supporting information[42] and varies from 5000 to 500 000. Each trajectory takes about 1.2 s of computer time on an IBM SP supercomputer with 375 MHz Power 3 WinterHawk+ processors, and it is worthwhile to note that for these weakly coupled systems, the fully converged quantum mechanical calculations (with our unique, highly optimized computer program) are less expensive than some of the well converged (with respect to the number of trajectories) semiclassical trajectory methods. Nevertheless, trajectory methods remain more easily programmable and affordable for large systems where accurate quantum dynamics become prohibitive, so it is important to test the reliability of the semiclassical methods.

The TFS-(−, +) method systematically overestimates the reaction and quenching probabilities for weakly coupled systems. [This is also true for the TFS-(−, −) and TFS-(+, +) methods. However, the choice of the "+" or "−" protocol is not important to the discussion in this and the next several paragraphs, and only the TFS-(−, +) method will be discussed.] We can explain the trend in P_R and P_Q by noting that in the 12 YRH cases studied here, 25%–80% of the TFS-(−, +) trajectories that finish the simulation on the lower electronic surface experience at least one frustrated hopping attempt. Trajectories that experience frustrated hopping attempts are trapped in the ground electronic state, leading to values of P_R and P_Q that are greater than the value demanded by the fewest-switches algorithm. We can estimate a lower limit on the TFS transition probabilities by considering only those trajectories that do not experience any frustrated hops. This is accomplished by the TFS-AFH method. The TFS-(−, +) result, the TFS-AFH result, and the quantum mechanical result for the reaction and quenching probabilities for the (1.10, 0) initial conditions are plotted in Fig. 3. For all four of the PEMs, the quantum mechanical transition probabilities are bracketed by the TFS-(−, +) and TFS-AFH results. For (1.10, 6) and (1.02, 0), this trend is observed for three of the four PEMs. The total nonadiabatic probability P_N, which was defined above as $P_R + P_Q$, is bracketed by the TFS-(−, +) result and the TFS-AFH result for all four PEMs in the YRH family and all three sets of initial conditions.

For the YRH systems, the likelihood that a trajectory will hop to the ground state twice is approximately equal to P_N^2, which is in most cases negligible compared to P_N. (Note that this is not true for the more strongly coupled MXH systems where multiple hopping trajectories are an important part of the nonadiabatic dynamics.) Therefore, for weakly coupled systems, the TFS-AFH result is not merely a lower limit on the TFS transition probabilities; the TFS-AFH result is approximately the result that would be obtained if every frustrated hopping attempt called for by the TFS algo-

rithm were allowed to occur. The fact that neither the TFS-(−, +) method nor the TFS-AFH method is accurate for the weakly coupled YRH systems motivates the search reported in this paper for a modification to the TFS method that allows some frustrated hops and removes (or ignores) others.

We note that the model YRH systems provide a dramatic example of the role that frustrated hopping plays in the sensitivity of TSH calculations to the choice of electronic representation. As previously mentioned, all of the semiclassical calculations reported in this paper were carried out in the adiabatic representation, except when noted otherwise. The model YRH(0.20) system and the initial conditions (1.10, 0), TFS-(−, +) calculations carried out in the diabatic representation [called the TFS-(−, +)-di method] predict reaction probabilities ten times greater and quenching probabilities four times greater than those predicted by the adiabatic TFS-(−, +) calculations. We note that ~97% of trajectories that finish the simulation in the lower diabatic state experience at least one frustrated hopping attempt, and that the quantum mechanical reaction and quenching probabilities (which are invariant to the choice of electronic representation) are bracketed by the TFS-(−, +)-di and the TFS-AFH-di methods, just as they are for the adiabatic results. We will not discuss the diabatic calculations further.

The symmetrized probability methods that weight the surfaces by $\frac{1}{2}$ significantly overestimate the reaction and quenching probabilities for the weakly coupled model YRH systems. We have previously discussed how frustrated hopping causes the TFS-(−, +) method to overestimate P_N. The symmetrized methods eliminate frustrated hopping, but do so in a way that increases the probability of transitions to lower-energy states and decreases the probability of transitions from lower-energy states to higher-energy states. This can be seen from Eqs. (9)–(16). For any of the symmetrized methods, b'_{kl} will be greater than the value of b_{kl} for the TFS-(Prot-L, Prot-E) methods given by Eq. (5) whenever the trajectory is in the higher-energy electronic state, and b'_{kl} will always be less than b_{kl} when the trajectory is in the lower-energy electronic state.

The more physical n_χ-weighted methods have much lower errors in the probabilities than the $\frac{1}{2}$-weighted methods. For the YRH systems, $n_1 \approx 0$ and $n_2 \approx 1$, so the value of b'_{kl} is nearly equal to b_{kl} when the trajectory is in the higher-energy electronic state. The value of b'_{kl} is not equal to b_{kl} when the trajectory is in the lower-electronic state, but multiple hopping trajectories are not important in determining the dynamics of the YRH systems. Therefore the value of b'_{kl} after a hop down to the lower-energy state is only important in determining whether or not the trajectory will experience a frustrated hop. In the n_χ-weighted methods, frustrated hops are eliminated, which has the same effect on the final observables as ignoring the frustrated hops, and the n_χ-weighted methods give similar results to the TFS-(+, +) method. The total nonadiabatic probability is systematically slightly higher than the TFS-(+, +) method due to the considerations discussed above for the $\frac{1}{2}$-weighted methods. Table III shows that the GC(n_χ) method (which is, overall, the most accurate of the symmetrized methods tested here) predicts less accurate values for P_N than any of the TFS-(Prot-L, Prot-E) methods.

It should also be noted that the symmetrized methods cannot be used in the diabatic representation because the diabatic coupling is not a function of the velocity of the classical trajectory. We also note that the functions presented in Eqs. (9)–(16) are not smooth functions, i.e., they have discontinuous first derivatives. This arises from the fact that while the trajectory is traveling on a single electronic surface, Eqs. (9)–(16) are functions of the velocity (or speed) of the trajectory on both electronic states. This speed for the unoccupied state does not correspond to a physical path of a trajectory traveling on the unoccupied electronic surface. For example, if on the occupied surface the trajectory experiences a turning point in one of its modes, the velocity in that mode will decrease, pass through zero, and increase from zero with a different sign. The velocity computed for the unoccupied surface will also switch signs, but it will not necessarily go through zero, resulting in discontinuities in the velocity in that mode and its derivative. These discontinuities can affect the efficiency of the trajectory calculation if the equations for a_{kl} are integrated with an algorithm that requires smooth derivatives.

We will now turn our attention to the TFS-(−, +), TFS-(+, +), TFS-(−, −), and TFS-(R, +) methods. The treatment of frustrated hops can have a significant effect on the final observables. The effect is greater for the weakly coupled YRH systems than for the more strongly coupled MXH systems, where multiple hopping trajectories are important. In general, the TFS-(+, +) method predicts the most accurate moments, the TFS-(−, −) method predicts the most accurate values of F_R, and the TFS-(R, +) method predicts the most accurate values of P_N.

Reflecting the nuclear momentum along **d** during a frustrated hop leads to increased error in the final moments and decreased error in the product branching ratio. We can explain the trend in F_R by noting that for the (1.10, 0) and (1.02, 0) sets of initial conditions, the reaction probability P_R for the TFS-(−, −) method is usually less than P_R calculated by the TFS-(+, +) method, whereas the total nonadiabatic probability P_N is relatively unchanged. The upper electronic state in the reactive arrangement is energetically inaccessible, leading to a large number of trajectories that experience energy forbidden hops as they are exiting this arrangement. In the TFS-(+, +) method, these frustrated hops are ignored, and the trajectories finish in the reactive arrangement. In the TFS-(−, −) method, trajectories with frustrated hopping attempts in this region are reflected in the direction of **d**, which has a large component parallel to the reactive channel. This causes some trajectories to be reflected back into the interaction region, lowering the value of P_R for the TFS-(−, −) method. For the (1.10, 6) set of initial conditions, the increased energy in the rotational modes leads to an increased number of momentum-forbidden hops in the quenching product arrangement. These trajectories are reflected back into the interaction region in the TFS-(−, −) method, lowering the value of P_Q relative to the TFS-(+, +) method. For all three sets of initial conditions, reflection of trajectories with frustrated hops back into the interaction re-

gion improves the agreement of the semiclassical value of F_R with the quantum mechanical result. However, the reflection along **d** also leads to increased errors in the final moments.

It is reasonable, therefore, to consider methods that combine the "+" and the "−" protocols, such as the TFS-(−, +) method. We have previously mentioned, however, that energy-forbidden and momentum-forbidden hops should be treated consistently. Our results indicate that the TFS-(−, +) method is not the best strategy for combining the two reflection protocols, and it leads to less accurate final moments and the product branching ratios than either the TFS-(+, +) method or the TFS-(−, −) method. It should also be noted that the **d** direction may not be the best direction in which to reflect the nuclear momentum during a frustrated hopping attempt when applying the "−" protocol.

We can draw a similar conclusion about the TFS-(R, +) method. The TFS-(R, +) method predicts the best values for the total nonadiabatic probability P_N. We can explain this for the YRH systems by observing that the quantum mechanical data lie between the TFS-(−, +) and the TFS-AFH data, as shown in Fig. 3. The TFS-(R, +) method allows a subset of frustrated trajectories (namely those trajectories with momentum-frustrated hops) to occur, improving the agreement of the semiclassical value of P_N with the quantum mechanical result. We note, however, that because the probability of hopping to the ground state twice is small, the trajectories that hop to the upper electronic state using the rotated **d** vector do not significantly affect the final reaction or quenching moments. In other systems where multiple hopping trajectories are important, the rotated hopping vector has a larger effect on the final moments, as observed in a previous study[12] and in the present study for the rotational moments of the more strongly coupled MXH systems.

Although it would be desirable for Tables III–V to show a clearly superior method, it is evident that a semiclassical method that successfully solves the problem of classically forbidden hops must be more sophisticated than the simple methods tested in this paper. We can, however, use the results of the present systematic study to suggest several important features that a method likely must have in order to successfully treat frustrated hops: (1) Some, but not all, frustrated trajectories should be reflected. (2) Some, but not all, frustrated hops should somehow be allowed to hop to the upper electronic state. (3) The criterion for reflection and the criterion for allowing classically forbidden hops should not be based on the partition of energy in modes orthogonal to **d**, i.e., energy-forbidden and momentum-forbidden hops should be treated consistently. (4) The use of symmetrized speed or coupling functions in the expression for the hopping probability systematically leads to increased reaction and quenching probabilities and thereby to worse agreement with accurate calculations; hence these methods are not recommended.

The choice of "best method" depends on the observable of interest, specifically: the TFS-(+, +) method performs best when calculating the final vibrational and rotational moments, the TFS-(−, −) method gives the best value for the reactive/nonreactive branching ratio F_R, and the TFS-(R, +) method gives the best electronically nonadiabatic transition probabilities. Although there is no method that is the best method for all observables, we see from Table V that, averaged over all observables, the TFS-(+, +) method is the most accurate of the semiclassical methods for modeling weakly coupled systems, where classically forbidden hops are a serious problem.

VII. CONCLUSIONS

We have presented fully converged quantum mechanical scattering calculations for four weakly coupled three-atom, two-state systems. The systems are fully three-dimensional and realistic. The systems are specifically designed to be weakly coupled systems where the frustrated hopping problem is most serious; if one is to make a recommendation about the best way to treat frustrated hopping, it is most appropriate to make that decision on the basis of studying systems where the various choices have the most significant impact on the results, i.e., systems where classically forbidden hops are an essential part of the problem.

We tested the TFS (Tully's fewest-switches) surface hopping method with three different sets of initial conditions for each of the four YRH PEMs, as well as with one set of initial conditions for a more strongly coupled set of three MXH PEMs. We have shown that for weakly coupled systems, the TFS method systematically overestimates the reaction and quenching probabilities due to the frequent occurrence of classically forbidden hopping attempts. We have explored several variants of the TFS method which differ in their treatment of frustrated hopping and have shown that the treatment of frustrated hopping has a large effect on the final nonadiabatic transition probabilities and the final vibrational and rotational moments. The effect of frustrated hops was shown here to be critically important for the correct treatment of systems with weakly coupled electronic states, and we know from previous work[12,14] and additional studies presented here that the treatment of frustrated hops is also significant for more strongly coupled systems.

The TFS-(R, +) method is shown to predict the best total nonadiabatic probabilities. The TFS-(+, +) scheme, which ignores all types of frustrated hops, predicts the best final vibrational and rotational moments, and the TFS-(−, −) method predicts the best product branching ratios. Averaged over all observables, the TFS-(+, +) method is the best of the semiclassical methods tested here. Although there is no method that completely solves the problem of classically frustrated hops, we have motivated the search for a more sophisticated protocol for the treatment of frustrated hops, and we have inferred several features that a successful method is likely to have.

We also tested eight symmetrized velocity and coupling methods. These methods were shown to be extremely ill suited for modeling the dynamics of weakly coupled systems when the coupling contributions from both surfaces were weighted equally. Weighting using the electronic state populations significantly increased the accuracy of the method, and the results of the best symmetrized method are only slightly less accurate, on the average, as those obtained using the best nonsymmetrized coupling method. However, the symmetrized methods are specialized to the adiabatic repre-

sentation, systematically increase the nonadiabatic transition probabilities, and can cause numerical difficulties in their implementation.

Although a major goal of this work was the comparison of various strategies for dealing with the frustrated hopping problem, we should not lose sight (in considering *relative* accuracy of the methods) of an important conclusion about *absolute* accuracy of multidimensional semiclassical methods in general for weakly coupled systems. This is the most extensive test ever carried out (superceding Ref. 13) for weakly coupled multidimensional semiclassical nonadiabatic methods for three-body collisions in full three-dimensional space, featuring new quantum mechanical results and over 12 mil trajectories. The accurate quantal values of the probability P_N of a nonadiabatic event (averaged over energy intervals of 0.06 eV) range from 3×10^{-5} to 1×10^{-1}, or, on a logarithmic scale, $\log_{10}P_N$ ranges from -4.5 to -1.0. And yet the five semiclassical methods that were applied to all 12 cases have mean unsigned errors in $\log_{10}P_N$ that range from 0.09 to 0.15 (corresponding to typical errors of only about 30%). Thus semiclassical methods are remarkably accurate even in these highly nonclassical weakly coupled systems. This provides strong confirmation of the value of past detailed studies of these methods, and it also validates their use for applications. Furthermore, it motivates the continuing search for further refining these methods so that other aspects of the results, for example, the probabilities of nonadiabatic reaction, may become equally accurate.

ACKNOWLEDGMENTS

This work was supported in part by the National Science Foundation under Grant Nos. CHE97-25965 and CHE00-92019.

APPENDIX: EHRENFEST METHOD

Although this paper is primarily concerned with studying the treatment of frustrated hopping in trajectory surface hopping calculations, we also tested the semiclassical Ehrenfest method[39,40] for all four YRH systems and all three sets of initial conditions, for a total of 12 cases. In the semiclassical Ehrenfest method, trajectories are propagated on a mixed potential energy surface which is a linear combination of the adiabatic surfaces weighted by the quantum mechanical state populations. The semiclassical Ehrenfest method predicts no reaction because mixing in even a small amount of the upper surface prohibits the system from reaching the product. However, we can still test the method for P_Q, $\langle\nu''\rangle$, $\langle j''\rangle$, and P_N.

Semiclassical Ehrenfest (SE) trajectories finish the simulation in a mixed stated in the Y+RH arrangement. The final state electronic state populations n_1 and n_2 are used to assign electronic probability density to the upper and lower surfaces. Here we test three different methods for assigning the electronic probability. In the SE-H method, the trajectory is assigned to the closest electronic surface. For the YRH(0.20) system, a small set of trajectories finish with a $n_1>0.5$. For the other PEMs, the SE-H method predicts zero quenching probability. The SE-LSS method assigns a weight of n_1 to the quenching probability. This method has errors comparable to the TFS methods for the quenching and total nonadiabatic probabilities and the final moments. The SE-QSS method assigns a weight of n_1^2 to the quenching probability if $n_1<n_2$ (which is usually the case) and a weight of $1-n_2^2$ if $n_1>n_2$. The results of the SE-QSS method are intermediate of the SE-LSS and the SE-H methods. Table VI gives MUEs of the semiclassical Ehrenfest methods.

TABLE VI. Mean unsigned errors in the semiclassical methods for quenching and nonadiabatic probabilities for the four YRH systems and three sets of initial conditions (12 cases).

Method	$\log_{10}P_Q$	$\langle\nu''\rangle$	$\langle j''\rangle$	$\log_{10}P_N$
TFS-(−,+)	0.11	0.36	2.20	0.13
TFS-(+,+)	0.10	0.22	1.92	0.11
TFS-(−,−)	0.13	0.38	2.19	0.13
TFS-(R,+)	0.13	0.25	2.14	0.09
SE-H[a]	1.12	0.03	1.79	1.21
SE-LSS	0.13	0.86	0.89	0.17
SE-QSS	1.67	0.88	1.29	1.75

[a]The Ehrenfest-histogram method does not predict any quenching for YRH(0.10), YRH(0.03), or YRH(0.01) at any of the initial conditions. The errors presented here are the average of the three initial conditions for the YRH(0.20) system.

[1] E. E. Nikitin, Annu. Rev. Phys. Chem. **50**, 1 (1999).
[2] E. E. Nikitin and S. Ya. Umanski, *Theory of Slow Atomic Collisions* (Springer-Verlag, Berlin, 1984).
[3] E. A. Gislason, G. Parlant, and M. Sizun, Adv. Chem. Phys. **82**, 321 (1992).
[4] H. Nakamura, Adv. Chem. Phys. **82**, 243 (1992).
[5] H. Nakamura, in *Dynamics of Molecules and Chemical Reactions*, edited by R. E. Wyatt and J. Z. H. Zhang (Marcel Dekker, New York, 1996), p. 473.
[6] J. C. Tully, in *Modern Methods for Multidimensional Dynamics Computations in Chemistry*, edited by D. C. Thompson (World Scientific, Singapore, 1998), pp. 34 and 72.
[7] M. D. Hack and D. G. Truhlar, J. Phys. Chem. A **104**, 7917 (2000).
[8] S. L. Mielke, G. J. Tawa, D. G. Truhlar, and D. W. Schwenke, Chem. Phys. Lett. **234**, 57 (1995).
[9] M. S. Topaler, M. D. Hack, T. C. Allison, Y.-P. Liu, S. L. Mielke, D. W. Schwenke, and D. G. Truhlar, J. Chem. Phys. **106**, 8699 (1997).
[10] M. S. Topaler, T. C. Allison, D. W. Schwenke, and D. G. Truhlar, J. Phys. Chem. A **102**, 1666 (1998).
[11] M. S. Topaler, T. C. Allison, D. W. Schwenke, and D. G. Truhlar, J. Chem. Phys. **109**, 3321 (1998).
[12] M. D. Hack, A. W. Jasper, Y. L. Volobuev, D. W. Schwenke, and D. G. Truhlar, J. Phys. Chem. A **103**, 6309 (1999).
[13] Y. L. Volobuev, M. D. Hack, and D. G. Truhlar, J. Phys. Chem. A **103**, 6225 (1999).
[14] M. D. Hack, A. W. Jasper, Y. L. Volobuev, D. W. Schwenke, and D. G. Truhlar, J. Phys. Chem. A **104**, 217 (2000).
[15] Y. L. Volobuev, M. D. Hack, M. S. Topaler, and D. G. Truhlar, J. Chem. Phys. **112**, 9716 (2000).
[16] M. D. Hack and D. G. Truhlar, J. Chem. Phys. **114**, 2894 (2001).
[17] M. D. Hack and D. G. Truhlar, J. Chem. Phys. (in press).
[18] L. D. Landau, Phys. Z. Sowjetunion **2**, 46 (1932); C. Zener, Proc. R. Soc. London, Ser. A **137**, 696 (1932); E. C. G. Stückelberg, Helv. Phys. Acta **5**, 369 (1932); E. Teller, J. Chem. Phys. **41**, 109 (1937).
[19] N. Rosen and C. Zener, Phys. Rev. **18**, 502 (1932).
[20] Yu. N. Demkov, J. Exp. Theor. Phys. **45**, 195 (1963) [Sov. Phys. JETP **18**, 138 (1964)]; Dokl. Akad. Nauk SSSR **166**, 1076 (1966) [Sov. Phys. Dokl. **11**, 138 (1966)].
[21] A. Bjerre and E. E. Nikitin, Chem. Phys. Lett. **1**, 179 (1967).
[22] R. K. Preston and J. C. Tully, J. Chem. Phys. **54**, 4297 (1971); J. C. Tully and R. K. Preston, *ibid.* **55**, 562 (1971).
[23] W. H. Miller and T. F. George, J. Chem. Phys. **56**, 5637 (1972).

[24] J. C. Tully, in *Dynamics of Molecular Collisions*, edited by W. H. Miller (Plenum, New York, 1976), Part B, pp. 217–267.
[25] D. G. Truhlar and J. T. Muckerman, in *Atom-Molecular Collision Theory*, edited by R. B. Bernstein (Plenum, New York, 1979), pp. 505–594.
[26] P. J. Kuntz, J. Kendrick, and W. N. Whitton, Chem. Phys. **38**, 147 (1979); G. Parlant and E. A. Gislason, J. Chem. Phys. **91**, 4416 (1989).
[27] N. C. Blais and D. G. Truhlar, J. Chem. Phys. **79**, 1334 (1983).
[28] M. F. Herman, J. Chem. Phys. **81**, 754 (1984).
[29] N. C. Blais, D. G. Truhlar, and C. A. Mead, J. Chem. Phys. **89**, 6204 (1988).
[30] J. C. Tully, J. Chem. Phys. **93**, 1061 (1990).
[31] P. J. Kuntz, J. Chem. Phys. **95**, 141 (1991).
[32] S. Chapman, Adv. Chem. Phys. **82**, 423 (1992).
[33] M. F. Herman, Annu. Rev. Phys. Chem. **45**, 83 (1994).
[34] U. Müller and G. Stock, J. Chem. Phys. **107**, 6230 (1997).
[35] J.-Y. Fang and S. Hammes-Schiffer, J. Phys. Chem. A **103**, 9399 (1999).
[36] J.-Y. Fang and S. Hammes-Schiffer, J. Chem. Phys. **110**, 11166 (1999).
[37] D. F. Coker and L. Xiao, J. Chem. Phys. **102**, 496 (1995).
[38] See endnote 39 in S. Hammes-Schiffer and J. C. Tully, J. Chem. Phys. **101**, 4657 (1994).
[39] C. Zhu, K. Nobusada, and H. Nakamura (to be published).
[40] H.-D. Meyer and W. H. Miller, J. Chem. Phys. **70**, 3214 (1979).
[41] A. García-Vela, R. B. Gerber, and D. G. Imre, J. Chem. Phys. **97**, 7242 (1992).
[42] See EPAPS Document No. E-JCPSA6-115-033125 for supporting information including: the functional form of the YRH model surfaces, the parameters of the quantum mechanical basis sets, the energy dependence of the quantum mechanical results, and the detailed results of the semiclassical trajectory calculations. This document may be retrieved via the EPAPS homepage (http://www.aip.org/pubservs/epaps.html) or from ftp.aip.org in the directory /epaps/. See the EPAPS homepage for more information.
[43] Y. Sun, D. J. Kouri, D. G. Truhlar, and D. W. Schwenke, Phys. Rev. A **41**, 4857 (1990).
[44] D. W. Schwenke, S. L. Mielke, and D. G. Truhlar, Theor. Chim. Acta **79**, 241 (1991).
[45] G. J. Tawa, S. L. Mielke, D. G. Truhlar, and D. W. Schwenke, J. Chem. Phys. **100**, 5751 (1994).
[46] G. J. Tawa, S. L. Mielke, D. G. Truhlar, and D. W. Schwenke, in *Advances in Molecular Vibrations and Collisional Dynamics*, edited by J. M. Bowman (JAI, Greenwich, CT, 1994), Vol. 2B, pp. 45–116.
[47] D. W. Schwenke, Y. L. Volobuev, S. L. Mielke *et al.*, VP-version 18.8, University of Minnesota, Minneapolis, MN, 1999.
[48] D. G. Truhlar, J. Abdallah, Jr., and R. L. Smith, Adv. Chem. Phys. **25**, 211 (1974).
[49] D. W. Schwenke, K. Haug, M. Zhao, D. G. Truhlar, Y. Sun, J. Z. H. Zhang, and D. J. Kouri, J. Phys. Chem. **92**, 3202 (1988).
[50] M. S. Topaler, M. D. Hack, Y. L. Volobuev, A. W. Jasper, T. C. Allison, T. F. Miller III, Y.-P. Liu, N. C. Blais, and D. G. Truhlar, NAT-version 6.0, University of Minnesota, Minneapolis, MN, 2000.
[51] D. G. Truhlar, B. P. Reid, D. E. Zurawski, and J. C. Gray, J. Phys. Chem. **85**, 7861 (1981).